The unshunted SQUID revisited

Mikko Kiviranta
VTT, Tietotie 3, 02150 Espoo, Finland

E-mail: Mikko.Kiviranta@vtt.fi

Abstract. We have demonstrated stable running-mode operation of a superconducting quantum interferometer whose Josephson junction shunts are capacitively blocked in order to cut the signal-band noise currents. The intrinsic energy resolution of 26 times the Planck's constant was reached, which is compared against a numerical estimate obtained in the noise downmixing picture.

1. Introduction

The two-junction superconducting quantum interferometers, dc SQUIDs, have evolved significantly during the decades since the invention of the device [1]. A lot of effort has been invested in reduction of the input noise temperature and energy resolution of the coupled dc SQUIDs, and their noise performance is now approaching the quantum limit at sub-kelvin temperatures. The improved performance has been striven by curing of parasitic resonances [2], enhancing the shunt cooling [3], finding readout techniques to cross the 'noise temperature gap' between the SQUID and the room-temperature amplifier [4], and by increasing the noise bandwidth $\omega_C = (L_{SQ}\, C_J)^{-1/2}$ determined by the SQUID loop inductance and the capacitance of the Josephson junctions. In 1995 Seppä [5] proposed an additional method to improve performance: cutting the dissipation-related noise currents by capacitors in series with the junction shunts. The resulting device is called the unshunted SQUID (un SQUID). Although the un SQUID has potential to reach lower noise temperature and lower power dissipation than a dc SQUID with same parameters, it has seldom been demonstrated in practice [6] (results reprinted in [7]). However, devices with similar layout have been used in a switching rather than continuously running mode, [8, 9] where stability issues are not as important. We present here a practical demonstration of the un SQUID in a regime where, unlike the high gain (hg) SQUID –like experiments [5, 6], no external dc resistor is required for stable operation.

2. Un SQUID characteristics and noise

The expected un SQUID voltage-to-current characteristics can be determined by Josephson dynamical simulation of the device, but one can qualitatively obtain them by subtracting a linear slope from the voltage-biased characteristics of an ordinary dc SQUID. The subtracted slope corresponds to the dc current which flows through the parallel connection of the shunt resistors in dc SQUIDs, but is capacitively blocked in un SQUIDs. The flux to-current characteristics are expected to be similar to the dc SQUID.

The expected noise performance has been assessed both analytically [10] and numerically [11] but it can be roughly understood in the picture where Johnson noise from the shunt resistors adds to the signal both directly and via downmixing due to the Josephson oscillation [12]. To illustrate, we have numerically simulated [13] the downmixing coefficients of the noise-optimal $\beta_C = 0.7$, $\beta_L = 1$ dc SQUID [14]. The coefficients are shown in Fig. 1. Small sinusoidal test currents I_ν and I_ϕ were injected (Fig. 2) at frequencies ω, $\omega_J \pm \omega$, $2\omega_J \pm \omega$, and $3\omega_J \pm \omega$ while the resulting baseband output current $I_{SQ}(\omega)$ was recorded. $\omega_J = 2\pi\, U_B / \Phi_0$ is the Josephson oscillation frequency at the bias voltage U_B. The ratios of the output currents to the test currents $a_k = I_{SQ} / I_\nu$ and $g_k = I_{SQ} / I_\phi$ were observed to be linear in amplitude and independent of the baseband frequency ω in the explored regime. The $k = 0$ indicates the baseband frequency and the index $k > 1$ the mixing via the k:th harmonic of the Josephson oscillation. The SQUID output current is then

$$I_{SQ} = a_0 I_\nu(\omega) + \Sigma_{k=1}^{\infty}\left[a_{k-} I_\nu(k\omega_J - \omega) + a_{k+} I_\nu(k\omega_J + \omega)\right] + g_0 I_\phi(\omega) + \Sigma_{k=1}^{\infty}\left[g_{k-} I_\phi(k\omega_J - \omega) + g_{k+} I_\phi(k\omega_J + \omega)\right] \quad (1)$$

When the injected currents at frequencies ω, $\omega_J \pm \omega$… are taken to be uncorrelated noise currents with the spectral density $S_{I\nu} = S_{I\phi} = 4\, k_B\, T / R_S$, the

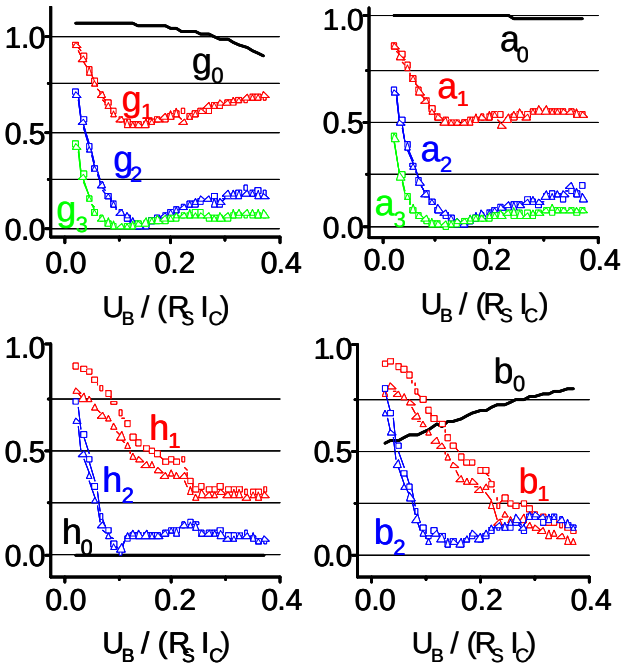

Figure 1: Simulated mixing coefficients of a voltage biased dc-SQUID from the ν - mode (a_k, h_k) and ϕ - mode excitations (b_k, g_k) into output current (a_k, g_k) and circulating current (b_k, h_k) responses. The mixing coefficients from the lower sideband a_{k-} … h_{k-} are indicated by squares, coefficients from the upper sideband a_{k+} … h_{k+} by triangles. The coefficients are evaluated as a function of the bias voltage U_B at the applied flux $\Phi_A = \Phi_0 / 4$.

sum (1) can be evaluated and expressed as the SQUID energy resolution

$$\varepsilon = \frac{S_{ISQ}}{2\left(dI/d\Phi\right)^2 L_{SQ}} = \frac{2 k_B T L_{SQ}}{R_S} \times \frac{\sum_{k=0}^{\infty} \left(a_{k\pm}^2 + g_{k\pm}^2\right)}{g_0^2} \,. \qquad (2)$$

The I_ν and I_ϕ represent in this case the sum and the difference of Johnson noise currents of the two shunt resistors and g_0 coincides with the ordinary SQUID gain $dI / d\Phi$. The optimum energy resolution obtained in this way for the dc SQUID (Fig. 2) is slightly lower than the $\varepsilon = 6.7\, k_B\, T\, L_{SQ} / R$ presented in [14]. In the un SQUID case the coefficients a_0 and g_0 do not contribute, resulting in a three times lower ε estimate.

We note that an expression similar to Eq. (1) can be constructed for the circulating current from the coefficients b_k, h_k (Fig 1). Again, the lack of signal band noise currents is expected to improve the back-action noise and consequently lead to a lower noise temperature in the un SQUID case.

3. SQUID construction

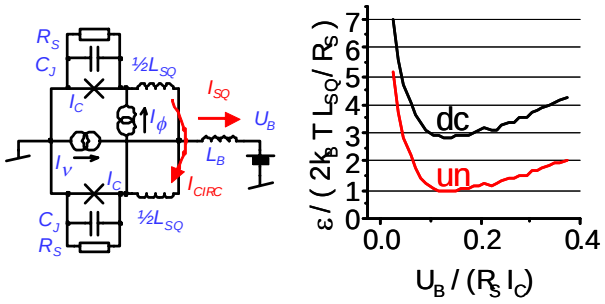

Figure 2: The circuit model used in simulation (left) and the energy resolution estimate obtained by square summing the four lowest downmixing coefficients a_0 … $a_{3\pm}$ and g_0 … $g_{3\pm}$ (right). The bias inductance $L_B = 40 \times L_{SQ}$ was used in the simulation.

The device tested here comes from a wafer fabricated in 2003 [15], but at the original critical current density $J_C = 1.2\times10^7$ A/m^2 its characteristics were 'growing hair' i.e. showing instability. We annealed some devices at 210 C for 90 min, which resulted in $J_C \approx 3\times10^6$ A/m^2 and more stable operation. The device layout and fabrication stack are depicted in Fig. 3, and the processing details are described in [15].

The SQUID loop is a 375 µm -diameter annulus divided into 12 parallel subloops. The calculated inductance due to the rim is 1.2 nH / 12^2 and due to the spokes 48 pH / 12, which matches reasonably well with the L_{SQ} = 11 pH obtained from the modulation depth of the unannealed large-J_C devices. Low ends of the Josephson junctions (JJs) in Fig. 3 connect to the NB1 wiring layer which also acts a the groundplane of the spokes. The left JJ connects to the NB2 layer where a set of 12 spokes lead to the loop rim, whereas the right JJ connects to the NB3 layer and another set of 12 spokes. Both spoke sets form microstrip transmission lines (TLs) w.r.t. the groundplane and the TLs terminate at 24 Ω resistors outside the rim. The parallel connection of 12 such resistors form each R_S = 2 Ω junction shunt shown in Fig. 4. The 150 pF Nb_2O_5-insulated capacitors are present at the rim, in series with each resistor. 12 such capacitors coupled in parallel form the C_S = 1.8 nF capacitors shown in Fig. 4.

One advantage of the multiloop construction is that it provides a flux transformer with an arbitrarily high turns ratio, which only contains narrow superconducting lines and therefore is less prone to flux trapping [16] than the washer-style transformer [17]. Another advantage is its potential for wideband coupling, in analogy with the Guanella transformer [18].

By moving the shunt resistors to the rim we combine them with the spoke microstrip

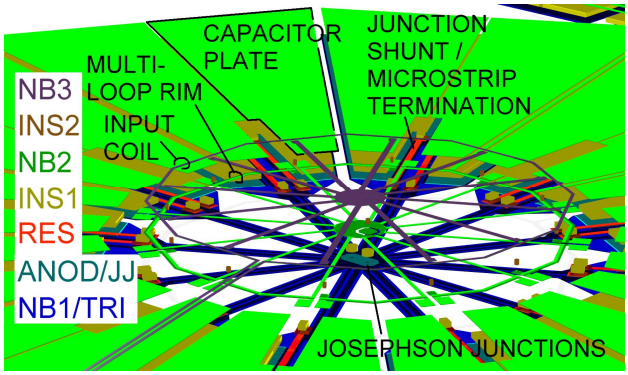

Figure 3: The 3D exploded view of the multiloop SQUID construction and the fabrication layers.

terminations in an attempt to reduce the total dissipation and therefore noise in the total circuit. Additionally, there is more space available for the electron-phonon coupling volume [3] of the shunt resistors and for the capacitors than there is close to the junctions.

We note that transmitting the Josephson oscillation power along the microstrip lines to be dissipated elsewhere is analogous to the photon-mediated heat conduction described by Meschke et al. [19]. The difference is that we excite only one electromagnetic mode (or a few modes), whereas Meschke et al. disperse the power over a bath of EM modes before conveying the power over the transmission line.

4. Experiments and discussion

Our experimental setup is sketched in Fig. 4. The un SQUID is coupled to an external damping circuit consisting of a R_E = 1 Ω SMD resistor and two Panasonic ECPU capacitors providing C_E = 0.66 μF. The voltage bias is created across the R_B = 0.1 Ω resistor. The un SQUID current is measured by a 480-SQUID array [20] which drives an INA163 instrumentation amplifier at room temperature. The array is operated without local linearization. The on-chip R_S-C_S circuit provides a voltage-like bias for the JJ ring down to 50 MHz above which the bond wires represent a significant parasitic reactance. The R_E-C_E circuit provides the bias condition down to ~250 kHz, above which the reactance of the array input L_I is too large.

The voltage-to-current and flux-to-current characteristics were measured with the array operated in a flux-locked loop. The results are shown in Figs. 5 and 6. The slope near the zero voltage in Fig. 5 is caused by the finite R_B and the resistance of the Cu wiring which connects the un SQUID to the SQUID array (Fig. 4).

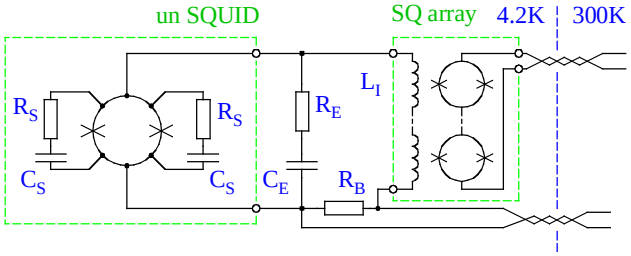

Figure 4: Simplified schematic of the readout circuitry.

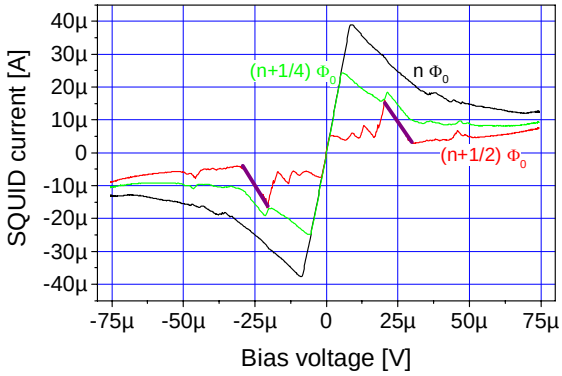

Figure 5: The current of the un SQUID as a function of the bias voltage, when applied flux is $n\,\Phi_0$, $(n+¼)\,\Phi_0$ and $(n+½)\,\Phi_0$. A thick line section indicates unstable region where the system oscillates at a few MHz.

The strongly distorted region at $U_B \approx 25$ μV corresponds approximately to the Josephson frequency at which the ~0.5 pF capacitance between the input coil and the multiloop rim tunes the ~1.2 nH input coil inductance. The fact that distortion is strongest in the $\Phi_A = (n+½)\,\Phi_0$ characteristics further suggests that the distortion is caused by some sort of a flux-mode resonance. In the distorted region the SQUID system is unstable and oscillates at a few MHz, which may just be the motorboating caused by a much higher instability frequency. At higher and lower bias voltages the system appears to be stable.

The flux noise level of $\Phi_N \approx 0.3$ μΦ$_0$ / Hz$^{1/2}$ was measured (Fig. 7) at $\Phi_A \approx \Phi_0/4$ and $U_B \approx 8$ μV, below which the finite biasing resistance us to reach the full modulation depth. This is well above the ~0.1 μΦ$_0$ / Hz$^{1/2}$ noise level resolvable by the readout array and the room temperature amplifier. The observed noise level is above even the dc SQUID theoretical optimum, and still farther from the un SQUID prediction (Fig. 2). However, the noise level is comparable with the modern coupled dc SQUIDs, a fact which suggests that the stable voltage biasing has been achieved over the full band

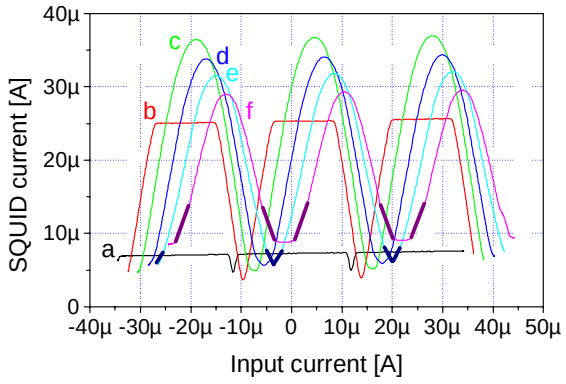

Figure 6: The current of the un-SQUID as a function of the flux-generating input coil current, at bias voltages (a) 1.8 μV, (b) 5.6 μV, (c) 8.5 μV, (d) 12 μV, (e) 15 μV and (f) 19 μV. A thick line section indicates unstable region. Each subsequent curve has been shifted by 2 μA in the flux direction, for the plot clarity.

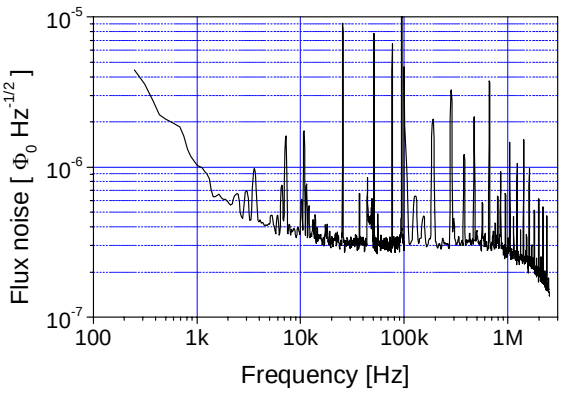

Figure 7: The measured flux noise of the un SQUID at T = 4.2 K.

from Josephson frequencies down to dc. Conceivable causes for the excess noise include the following: (i) the estimated parameters $\beta_C \approx 0.1$ and $\beta_L \approx 0.2$ of the annealed device are far from the noise optimum. (ii) The observed flux-mode resonance or other resonances in the transmission line structures cause excess noise. (iii) The resistance of the Pd shunts has deteriorated during the annealing step, an effect we have observed elsewhere [20]. Note that unlike in dc SQUIDs the shunt resistance variation cannot be easily observed from the voltage-current characteristics, hence determination of the realized R_S would require an experiment with a separate (similarly annealed) test resistor. The used bias voltage corresponds to $U_B \approx 0.2\ R_S\ I_C$ assuming that shunt resistors have not changed during the anneal step.

5. Conclusion

We have demonstrated stable biasing and readout of a coupled two-junction SQUID with frequency dependent damping, when the SQUID is operated in the continuously running mode. Such a device is called the un SQUID. The obtained intrinsic energy resolution ε = 26 h at 4.2 K falls short of theoretical predictions, but is good enough to indicate that there is nothing fundamentally wrong in the SQUID operation.

In addition, we have computed numerically the downmixing coefficients from the Josephson dynamics simulation which suggest that the energy resolution $\varepsilon \approx 2\ k_B\ T\ L_{SQ} / R_S$ is obtainable for the un SQUID, whereas the ordinary dc SQUID remains at $\varepsilon \approx 6\ k_B\ T\ L_{SQ} / R_S$.

Acknowledgement

This work has been supported by the Center of Excellence of the Finnish Academy of Sciences. We are indebted to Prof. Heikki Seppä who has conceived all the basic ideas behind the un SQUID. Thanks are due to Mr. Harri Pohjonen for annealing the devices and to Dr. Juha Hassel for checking the manuscript.

References

[1] Jaklevic R C, Lambe J, Silver A H and Mercreau J E 1964 Quantum interference effects in Josephson tunneling *Phys. Rev. Lett.* **12** 159-60.
[2] Seppä H and Ryhanen T 1987 Influence of the signal coil on dc-SQUID dynamics *IEEE Tran. Magn.* **23** 1083-6.
[3] Wellstood FC 1988 Excess noise in the dc SQUID; 4.2K to 20 mK *PhD Thesis* UC Berkeley.
[4] Drung D 2003 High-Tc and low-Tc dc SQUID electronics *SuST* **16** 1320-36.
[5] Seppä H, Kiviranta M and Grönberg L 1995 Dc SQUID Based on Unshunted Josephson Junctions: Experimental Results *IEEE Tran. Appl. Supercond.* **5** 3248-51.
[6] Seppä H et al. 1997 Experiments with a un SQUID based integrated magnetometer *Extended Abstracts of 6th Intl. Superconductive Electronics Conference (ISEC'97)* 26-8.
[7] Kiviranta M et al. 2003 Dc and un SQUID's for Readout of ac-Biased Transition-Edge Sensors *IEEE Tran. Appl. Supercond.* **13** 614-7.
[8] Robertson T L et al. 2005 Superconducting quantum interference device with frequency-dependent damping: Readout of flux qubits *Phys. Rev. B* **72** 024513.

[9] Hassel J et al. 2006 Rapid single flux quantum devices with selective dissipation for quantum information processing *APL* **89** 182514.
[10] Seppä H 2000 Ultimate limitation of the SQUID magnetometer *Proceedings of the 12th International Conference on Biomagnetism (Biomag 2000)* Ilmoniemi R J and Katila T, editors.
[11] Kiviranta M and Seppä H 1998 Noise simulation of the un SQUID *Applied Superconductivity* **6** 373-8.
[12] Likharev K K and Semenov V K 1972 *JETP Letters* **15** 442-5.
[13] The APLAC circuit simulator, http://web.awrcorp.com .
[14] Ryhänen T, Seppä H, Ilmoniemi R and Knuutila J 1989 SQUID magnetometers for low-frequency applications *J. Low Temp. Phys* **76** 287-386.
[15] Kiviranta M et al. 2004 Design and performance of multiloop and washer SQUIDs intended for sub-kelvin operation *SuST* **17** S285-9.
[16] Stan G, Field S. B. and Martinis J. M. 2004 Critical Field for Complete Flux Expulsion in Narrow Superconducting Strips *PRL* **92** 097003 .
[17] Jaycox J M and Ketchen M B 1981 Planar coupling scheme for ultra low noise dc SQUIDs *IEEE Tran. Magn.* **17** 400-3.
[18] Guanella G 1944 New method of impedance matching in radio frequency circuits *Brown-Boveri Review* **31** 327-9.
[19] Meschke M, Guichard W and Pekola J P 2006 Single-mode heat conduction by photons *Nature* **444** 187-90.
[20] Kiviranta M and Grönberg L 2009 Progress towards large locally linearized SQUID arrays *AIP Conf. Proc.* **1185** 526-9 .